Geographical features of changes in surface shortwave irradiance in East Asia estimated using the potential radiative forcing index

K. Kawamoto[1] and T. Hayasaka[2]

1 Faculty of Environmental Studies, Nagasaki University, Nagasaki, Japan

2 Center for Atmospheric and Oceanic Studies, Tohoku University, Sendai, Japan

Abstract

Using a recently-proposed index of the potential radiative forcing (PRF), we quantified 2-dimentional relative contributions of atmospheric parameters (clouds, aerosols and precipitable water) on the change of surface shortwave irradiance (*S*) over East Asia in July from 2003 to 2004. Analyses at some points revealed that contributions of the cloud optical depth, cloud amount and aerosol optical depth took various values, including the sign, depending the combination of atmospheric parameters' values and differences. The contribution of precipitable water was rather small compared to other parameters'. For example, the *S* change of totally about –70 (W/m^2) was estimated in the south China case because of all the negative factors. On the other hand, the *S* change of nearly 20 (W/m^2) was calculated as a result of a small negative aerosol effect and a moderate positive effect by the cloud optical depth in the central China case. Like these cases, PRF is useful in determining which of the parameters has a dominant effect on the overall change in *S*. Comparison of the summation of each PRF-derived contribution and the difference in *S* from the ISCCP products were fairly favorable (the correlation coefficient of 0.84). Regardless of a few shortcomings, obtained results demonstrated the usefulness of PRF for various climate investigations. Nonetheless, rigid validation against estimated *S* changes using PRF should be done with independent observations such as ground-based pyranometer measurements.

1. Introduction

The radiation budgets at both the surface and top of atmosphere (TOA) are important components of the Earth's climate. In particular, the surface shortwave irradiance (*S*) largely determines evapotranspiration and has a considerable effect on the dynamical process though absorption by ocean and land surfaces. The ground albedo and atmospheric parameters such as clouds, aerosols and water vapor influence *S*. Since these atmospheric parameters change temporally and spatially, their effects on *S* are complicated.

Changes in *S* have already received detailed investigation. The so-called solar dimming and brightening phenomenon, whereby *S* decreased for several decades before approximately 1990 and has since increased, has received a great deal of attention [e.g., Gilgen et al., 1998; Stanhill and Cohen, 2001; Wild et al., 2005], although the reason for this long-term change has not yet been determined. A study by Qian et al. [2006] revealed a downward trend in *S* between 1960 and 1990 over China, but this trend was inconsistent with decreases in cloud amount over most parts of China [Kaiser, 1998]. A modeling approach with the emission inventory has since been adopted to acquire a better understanding of the underlying principles [Streets et al., 2006].

Recently, Kawamoto and Hayasaka [2008; hereafter referred to as KH2008] defined an index of potential radiative forcing (PRF) to quantify the relative contributions of atmospheric parameters (clouds, aerosols, and water vapor) to change in *S* in East Asia; however, that study did not offer an explanation of the phenomena. PRF is defined as the sensitivities of *S* to differential increases from given values of the cloud optical depth, cloud amount, aerosol optical depth and precipitable water. The aim of this study is to quantify the relative contributions of each atmospheric parameter on the *S* change with two-dimension using PRF, extending KH2008. That is, how much *S* change is attributed by, for example, the cloud optical depth change? To answer this question, we performed following analyses.

Derivation and characteristics of PRF are briefly described in section 2, and geographical (two-dimensional) analyses are performed in section 3, and finally concluding

remarks are given in section 4.

2 Description of PRF

Surface shortwave irradiance (0.2-5 μm) of the considered point is determined by various factors such as clouds, aerosols, water vapor and the ground albedo, according to the solar incidence. We assume that S is formulated for a non-reflecting surface in the following equation:

$$S = S_0\left[(1-A_c)T_a + A_cT_c\right] \ , \tag{1}$$

where S_0 is the incident solar irradiance at the top of the atmosphere, which varies with the season and latitude and corresponding to the Earth's orbit and solar activity, and T_a and T_c are transmittances under cloud-free- and cloudy-sky conditions, respectively. The cloud-free-sky is defined as a condition with aerosols, water vapor and no clouds. The total cloud amount A_c is defined as the fraction occupied by cloudiness. The differential of Eq. (1) is obtained as follows:

$$\Delta S = S_0\left[(1-A_c)\Delta T_a + A_c\Delta T_c + (T_c - T_a)\Delta A_c\right] \ . \tag{2}$$

The Equation (2) indicates cloud-free and cloudy factors do not independently affect the change in S. For example, if A_c is large, the change in T_c substantially influences S, but the change in T_a does not have a large effect on S. The sensitivities of S to differential change of each parameter (cloud optical depth τ_c, aerosol optical depth τ_a, water vapor amount w and A_c) which were defined as the potential radiative forcing (PRF), are expressed as follows:

$$\frac{\partial S}{\partial \tau_c} = S_0 A_c \frac{\partial T_c}{\partial \tau_c} \ , \tag{3}$$

$$\frac{\partial S}{\partial \tau_a} = S_0\left[(1-A_c)\frac{\partial T_a}{\partial \tau_a} + A_c\frac{\partial T_c}{\partial \tau_a}\right] \ , \tag{4}$$

$$\frac{\partial S}{\partial w} = S_0\left[(1-A_c)\frac{\partial T_a}{\partial w} + A_c\frac{\partial T_c}{\partial w}\right] \ , \tag{5}$$

$$\frac{\partial S}{\partial A_c} = S_0(T_c - T_a) \ . \tag{6}$$

The expected change in S due to one parameter is obtained as the product of PRF and the change in that parameter. PRFs are calculated by the unit optical depth for τ_c and τ_a, 1% for A_c, and 1 mm for w in this study. As evident from the above equations, the PRFs depend on a combination of the values of the parameters and S_0 according to A_c. The value of PRF is always negative and becomes stronger (i.e., has a stronger influence on S) when the values of the atmospheric parameters are small and S_0 is large. Here, 'strong' and 'weak ' denote 'large (more negative)' and 'small (less negative)' of absolute values of PRFs. For all the radiation calculations in this study, we used a general radiative transfer code, *RSTAR*-5b, which solves the radiative transfer with a combined discrete-ordinate/matrix-operator method [Nakajima and Tanaka, 1986, 1988] with Lowtran-7 gas absorption model [Kneizys et al., 1988]. Climatology between 2002 and 2005 was used as input datasets for τ_c at visible wavelength, A_c and w from International Satellite Cloud Climatology Project (ISCCP) datasets [Rossow and Duenas, 2004], τ_a at 0.55 μm from Moderate Resolution Imaging Spectroradiometer (MODIS) products [Kaufman et al., 2002]. Values of T_a and T_c were calculated with changing τ_c, τ_a and w using this radiation code, and then PRFs were obtained together with A_c as formulated in eqs. (3)-(6). As for other minor constituents such as ozone, carbon dioxide and methane, we used their climatology in radiative transfer calculations, but did not investigate the effects of their changes on S in this study. Other detailed description on PRF was given in KH2008.

3. Results

KH2008 defined the PRF and concluded the usefulness for the earth radiation budget study, applying it to one point measurement at Jinan (117.0°N, 36.7°E). Here we estimated the two-dimensional geographical relative contribution of atmospheric parameters to the S change in July from 2003 to 2004 using PRF with meteorological products described in 3.1-3.5. The one year time period was due to more appropriateness of the parameters' linear change assumption during the period considered. In this section, using the PRF index, we

describe the geographical features of differences in atmospheric parameters, of PRF, and of differences in *S* due to those parameters. The mean geographical features of the atmospheric parameters under consideration during the time period used to develop the PRFs have been described by KH2008.

3.1 Datasets used

Although some studies used the annual mean values to investigate the radiation budget, we performed analyses with monthly mean datasets due to the large seasonal change. Target area was the East Asia region including China (75°E–135°E, 20°N–55°N) with 2.5° spatial resolution following KH2008. Only July was analyzed in this study. Data sources of clouds, aerosols and precipitable water were the same as ones we used in deriving PRFs.

3.2 Cloud optical depth

For changes of τ_c (Fig.1a), increases were observed in the south (particularly Fujian and Guangdong Provinces) and the west of the region, and the Korean Peninsula. Decreases were observed in the northeast of the region and near Japan. For PRF (Fig.1b), inland desert and mountainous areas had especially strong PRFs due to optically thin clouds. The same features applied over the East China Sea. Other parts were relatively weak, for example, the south and the Korean Peninsula owing to moderately thick clouds. Accordingly, *S* changes due to τ_c (Fig.1c) were negative in the south and west of the region and positive in the northeast of the region and Japan, respectively. An increase approximately 25 (W/m^2) around western Mongolia was due to slight decrease in τ_c and strong PRF.

3.3 Cloud amount

The values of A_c (Fig.2a) decreased in most parts of the north and near Japan, and increased in the small part of southern China. In particular, decreases near Japan were as

much as –25 W/m^2. In figure 2b, values of PRF were strong in the southwest and northeast. As a result, the change in S due to A_c, shown in figure 2c, was positive in the north, particularly near Japan, and negative in the south. Comparatively large decreases around Myanmar and southern Tibet were owing to strong PRF regardless of moderate increases in A_c.

3.4 Aerosol optical depth

The values of τ_a (Fig.3a) increased in southern China and in notably in northeastern India and decreased in several parts in the north and central areas. A decrease over the Lake Baikal was remarkable. PRF values (Fig.3b) were stronger over the north (particularly western Mongolia) and the East China Sea compared to other parts. For S change due to τ_a (Fig.3c), decreases in northeast India and southeast China in spite of less strong PRF were due to considerable increase in τ_a. Remarkable increase in the north (near the Lake Baikal) was the result of multiplication by the τ_a decrease and strong PRF. If a decrease in τ_a occurred over western Mongolia, the increase in S would be much greater.

3.5 Precipitable water

Values of w (Fig.4a) exhibited overall decreases in Tibet and northeast India and increases from the Japan Sea. Gentle increases were also found in north China. PRF values (Fig.4b) were generally weak compared to those of other parameters', but were stronger in Tibet. The S changes (Fig.4c) indicated positively around Tibet and negatively in northeastern China. An increase in S over Tibet was enhanced by a w decrease and stronger PRF. Contribution of w were, however, generally smaller than other parameters' over the region.

3.6 Analyses of the total S changes

Figure 5 shows the summation of PRF-derived *S* changes due to τ_c, A_c, τ_a and *w* in July from 2003 to 2004. We observed decreases over the south of the region (particularly the southern China) and the Korean Peninsula, and increases over the northeast of the region, Japan and the East China Sea. On the other hand, Figure 6 presents the difference in *S* for the same period from the ISCCP datasets. Geographical distributions of figures 5 and 6 were quite similar each other. A remarkable increase was observed over the Lake Baikal only for Fig. 5. This was attributed by an increase in PRF-derived *S* associated with a decrease in τ_a. ISCCP adopted an aerosol climatology calculated from the NASA/GISS climate model to obtain *S*, and difference between this modeled aerosol climatology and the MODIS aerosol product needs to be checked for this discrepancy.

Using the analyses above, figure 7 illustrates the relative contributions of atmospheric parameters on the *S* changes for the following three points: southern China (s), East China Sea (e) and mid China (m) as denoted by circles in Fig. 5. Contributions of the cloud optical depth, cloud amount and aerosol optical depth took various values, including the sign, depending the combination of atmospheric parameters' values and differences. The contribution of *w* was quite small in all cases, as the Jinan case in KH2008.

Figure 8 plots a comparison of the *S* changes between the ISCCP product and PRF-derived values (using figs. 5 and 6) with a fitted equation (red dotted line). The number of total samples was 336. The slope and intercept of the equation were 0.92 and 4.39, respectively. The root mean square was 18.4 (W/m^2). The agreement of both values seemed fairly good and the correlation coefficient (r) was 0.84 regardless of deviations like the Lake Baikal case. KH2008 and the current work assumed the imaginary part of aerosol complex refractive index (k_i) which determined absorptivity to be 0.02, since it is difficult to determine k_i from satellite remote sensing techniques. According to the general circulation model simulations by Takemura et al. [2002], the aerosol single scattering albedo (SSA) took about from 0.92 to 0.97 over East Asia, which corresponded roughly from 0.014 to 0.005, respectively for k_i, depending on particle size distributions and chemical species. Thus the currently assumed value of 0.02 was somewhat larger than the model outputs. As KH2008 suggested, the aerosol absorption property is important for

accurate evaluation of the radiation budget. Incorporating more realistic aerosol absorptivity from model outputs and/or observations would be an emergent task. There are always uncertainties in the cloud, aerosol and water vapor properties retrieved from satellite observations. The accuracy of the computed PRF depends on the accuracy of these satellite products. RRF are derived mainly from these products, thus estimated *S* change will be influenced by the uncertainty. Especially over arid regions with a high surface reflectivity, the uncertainty of retrievals is expected to be large. Furthermore, thin clouds are always difficult to retrieve from satellite observations over all types of surface. In these cases, the uncertainty in the estimated *S* change would be larger.

4. Concluding Remarks

4.1 Summary

This study determined the relative contributions of atmospheric parameters (clouds, aerosols, and water vapor) to change in *S* in East Asia (with 2.5° spatial resolution) between July 2003 and 2004 using the PRF index to quantify the sensitivity of *S* to differential changes in atmospheric parameters. The ISCCP and MODIS monthly products were used for inputs. Geographical features of contributions due to each atmospheric parameter to the *S* change were described, together with those of differences in parameters and of PRF. For example, the *S* change of totally about –70 (W/m^2) was estimated in the south China case because of all the negative factors. On the other hand, the *S* change of nearly 20 (W/m^2) was calculated as a result of a small negative aerosol effect and a moderate positive effect by the cloud optical depth in the central China case. Like these cases, PRF is useful in determining which of the parameters has a dominant effect on the overall change in *S*.

Comparison of the summation of each PRF-derived contribution and the difference in *S* from the ISCCP products were fairly favorable, showing the correlation coefficient was 0.84. These results demonstrated the usefulness of PRF for various climate investigations, specifically, coupling studies of the radiation budget with dynamical processes [Yuan et el.,

2008] and radiation-oriented GCM modeling efforts [e.g., Mukai et al., 2008].

4.2 Future work

As also raised in KH2008, a few shortcomings were, however, apparent in this approach. For example, 1) A single value of k_i was assumed over the region considered, although k_i can vary widely over China [Yu et al., 2006]. Effect of aerosol absorption cannot be negligible even under cloudy skies when absorptive [Hayasaka et al., 2006]. More realistic aerosol absorptivity should be incorporated in computing PRF. 2) Feedbacks among clouds, aerosols water vapor, and any relevant factors were not included. For instance, the aerosol indirect effects are too uncertain to take in the current formulae. Moreover, there would even exist other unidentified feedback processes and mechanisms.

Although only shortwave is currently treated, longwave is also important for the comprehensive understanding of the radiation budget. All the wavelengths including longwave need to be investigated. Rigid validation against estimated *S* changes using PRF should be done with independent observations. Shi et al. [2008] performed the quality check of long-term ground-based pyranometer measurements. These datasets are suitable for this purpose.

Acknowledgement

One of the authors (K. K.) was supported by a Japan Society for the Promotion of Science (JSPS) grant-in-aid for scientific research (C) and the President's discretionary funds of Nagasaki University. We used atmospheric and surface products provided by the ISCCP and MODIS science teams.

References

Gilgen, H., M. Wild, and A. Ohmura, 1998. Means and trends of shortwave incoming radiation at the surface estimated from Global Energy Balance Archive data, *J. Climate,* **11,**

2042–2061.

Hayasaka, T., K. Kawamoto, G. Shi, and A. Ohmura, 2006. Importance of aerosols in satellite-derived estimates of surface shortwave irradiance over China, *Geophys. Res. Lett.*, **33**, L06802, doi:10.1029/2005GL025093.

Kaiser, D.P., 1998. Analysis of total cloud amount over China. *Geophys. Res. Lett.* 25(19):3599-3602.

Kaufman, Y. J., D. Tanré, and O. Boucher, 2002. A satellite view of aerosols in the climate system, *Nature*, **419**, 215-223.

Kawamoto, K., and T. Hayasaka, 2008. Relative contributions to surface shortwave irradiance over China: A new index of potential radiative forcing, *Geophys. Res. Lett*., 35, L17809, doi:10.1029/2008GL035083.

Kneizys, F. X., E. P. Shettle, L. W. Arbeu, J. H. Chetwynd, G. P. Anderson, W. O. Gallery, J. E. A. Selby, and S. A. Clough, 1988. Users guide to LOWTRAN-7. *Air Force Geophysics Laboratory Tech. Rep*. AFGL-TR-88-0177, 137pp.

Mukai, M., T. Nakajima, T. Takemura, 2008. A study of anthropogenic impacts of the radiation budget and the cloud field in East Asia based on model simulations with GCM. *J. Geophys. Res*.,113, D12211, doi:10.1029/2007JD009325.

Nakajima, T., and M. Tanaka, 1986. Matrix formulations for the transfer of solar radiation in a plane-parallel scattering atmosphere. *J. Quant. Spectrosc. Radiant. Transfer*, 35, 13-21.

Nakajima, T., and M. Tanaka, 1988. Algorithms for radiative intensities calculations in moderately thick atmospheres using a truncation approximation. *J. Quant. Spectrosc.*

Radiant. Transfer, 40, 51-69.

Qian, Y., D.P. Kaiser, L.R. Leung, and M. Xu, 2006. More frequent cloud-free sky and less surface solar radiation in China from 1955–2000, *Geophys. Res. Lett.*, **33**, L01812, doi:10.1029/2005GL024586.

Rossow, W. B., and E. N. Duenas, 2004. The International Satellite Cloud Climatology Project (ISCCP) Web site - An online resource for research, *Bull. Am. Meteorol. Soc*., **85**, 167-172.

Shi, G.-Y., T. Hayasaka, A Ohmura, Z.-H. Chen, B. Wang, J.-Q. Zhao, H.-Z. Che, and L. Xu, 2008. Data quality control and the long-term trend of ground solar radiation over China, *J.Appl. Meteorol. Climatol.*, **47**, 1006-1016.

Stanhill, G., and S. Cohen, 2001. Global dimming: a review of the evidence for a widespread and significant reduction in global radiation with discussion of its probable causes and possible agricultural consequences, *Agric. for Meteorol.* 107, 255-278.

Streets, D. G., Y. Wu, and M. Chin, 2006. Two-decadal aerosol trends as a likely explanation of the global dimming/brightening transition, *Geophys. Res. Lett*., 33, L15806, doi:10.1029/2006GL026471.

Takemura, T., T. Nakajima, O. Dubovik, B. N. Holben, and S. Kinne, 2002. Single-scattering albedo and radiative forcing of various aerosol species with a global three-dimensional model. *J. Climate*, **15**, 333-352.

Wild, M., et al., 2005. From dimming to Brightening: Decadal changes in solar radiation at Earth's surface, *Science*, **308**, 847-850.

Yu, X., T. Cheng, J. Chen, and Y. Liu, 2006. A comparison of dust properties between China continent and Korea, Japan in east Asia, *Atmos. Environ*., 40, 5787–5797.

Yuan, J., D. L. Hartmann, R. Wood, 2008. Dynamic effects on the tropical cloud radiative forcing and radiation budget. *J. Climate*, **21**, 2337-2351.

Figure captions

Figure 1a Geographical distribution of τ_c change (no dimensions).

Figure 1b Geographical distribution of PRF due to τ_c (W/m^2).

Figure 1c Geographical distribution of *S* change due to τ_c (W/m^2).

Figure 2a Geographical distribution of A_c change (%).

Figure 2b Geographical distribution of PRF due to A_c ($W/m^2/\%$).

Figure 2c Geographical distribution of *S* change due to A_c (W/m^2).

Figure 3a Geographical distribution of τ_a change (no dimensions).

Figure 3b Geographical distribution of PRF due to τ_a (W/m^2).

Figure 3c Geographical distribution of *S* change due to τ_a (W/m^2).

Figure 4a Geographical distribution of *w* change (mm).

Figure 4b Geographical distribution of PRF due to *w* ($W/m^2/mm$).

Figure 4c Geographical distribution of *S* change due to *w* (W/m^2).

Figure 5 Geographical distribution of the summation of PRF-derived *S* changes due to τ_c, A_c, τ_a and *w* (W/m^2).

Figure 6 Geographical distribution of the difference in *S* from the ISCCP products (W/m^2).

Figure 7 Relative contributions of atmospheric parameters on the *S* changes for southern China, East China Sea and mid China.

Figure 8 Comparison of the *S* changes between the ISCCP product and PRF-derived values together with a regression line.

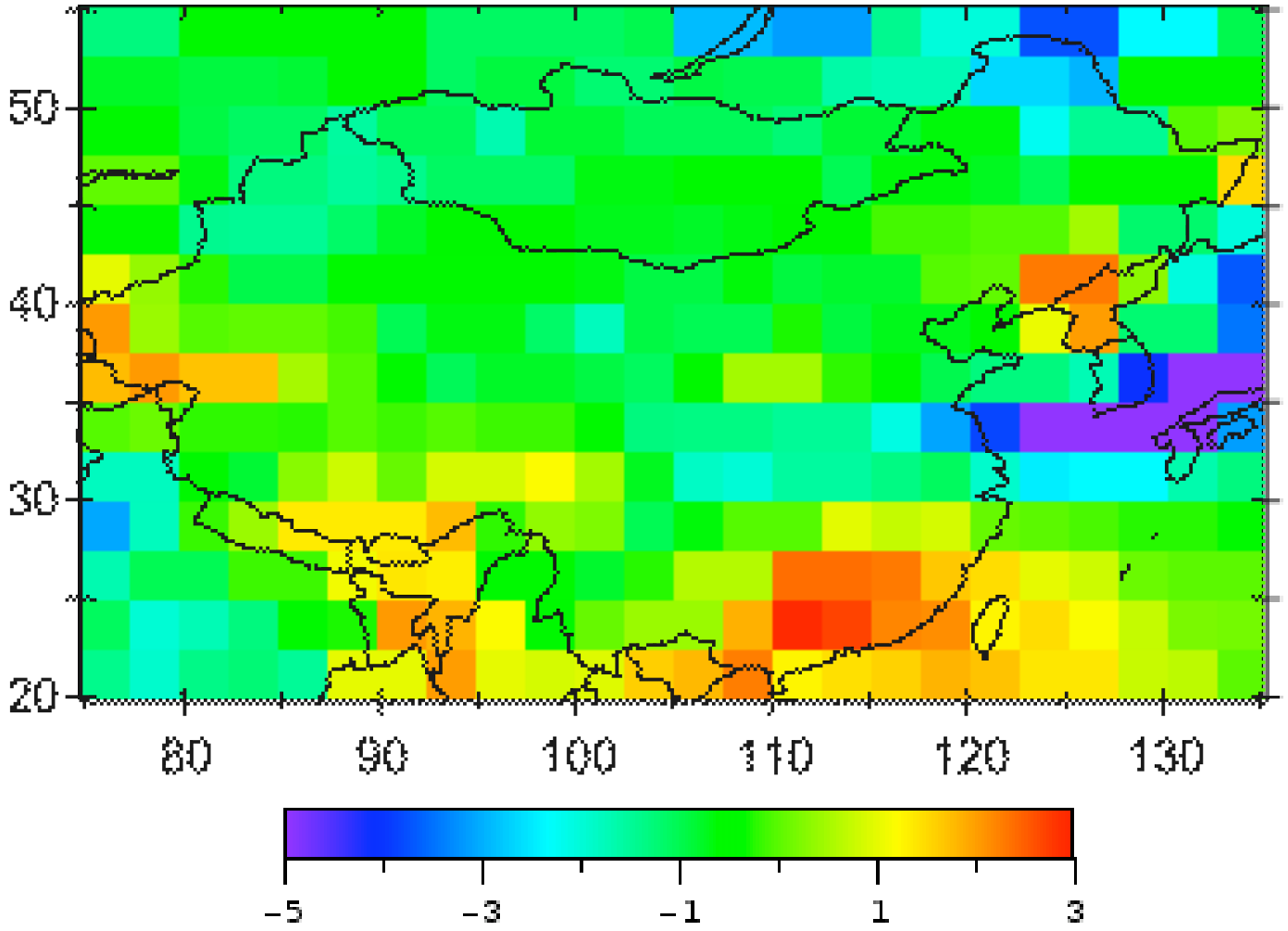

Figure 1a

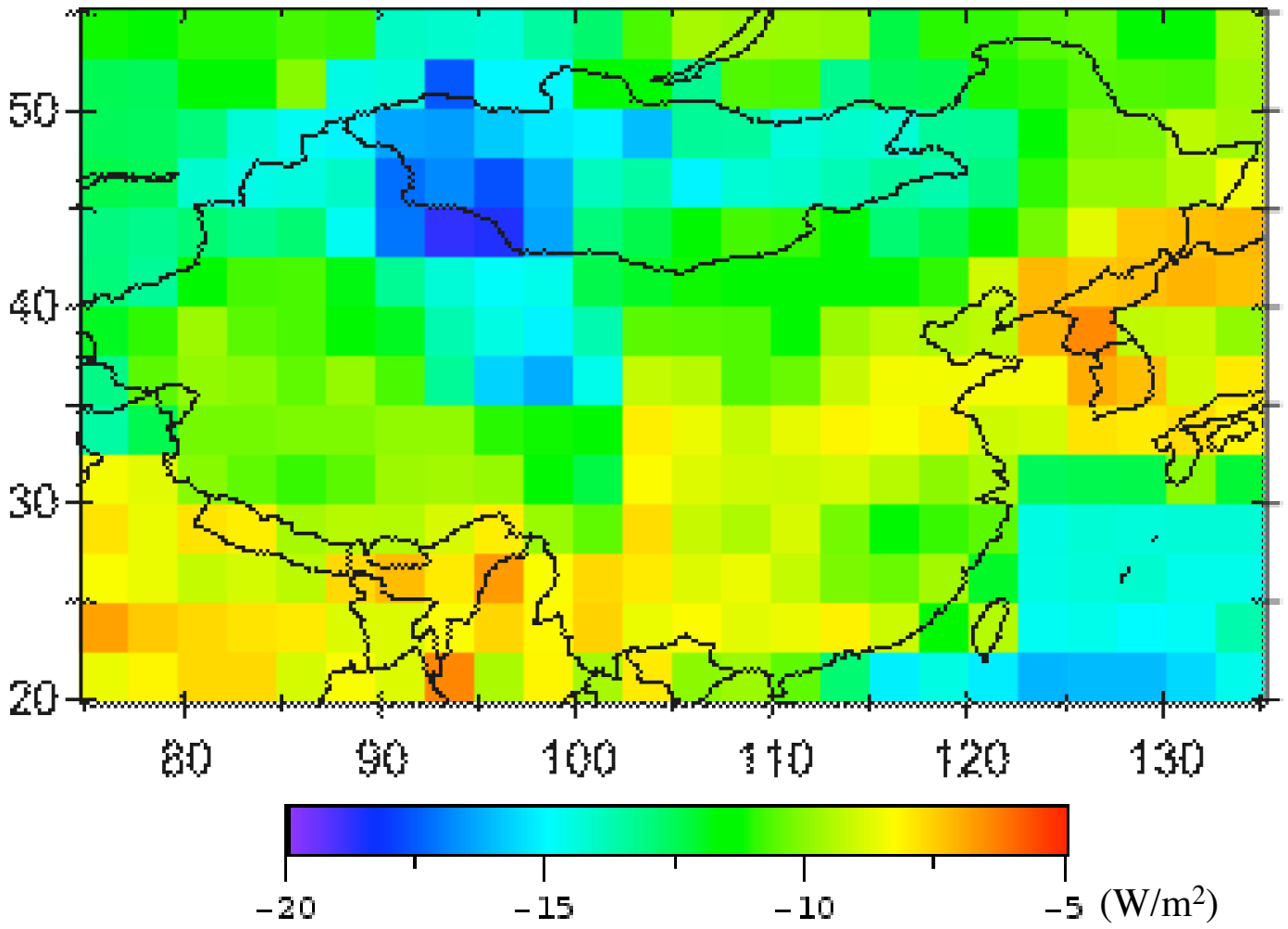

Figure 1b

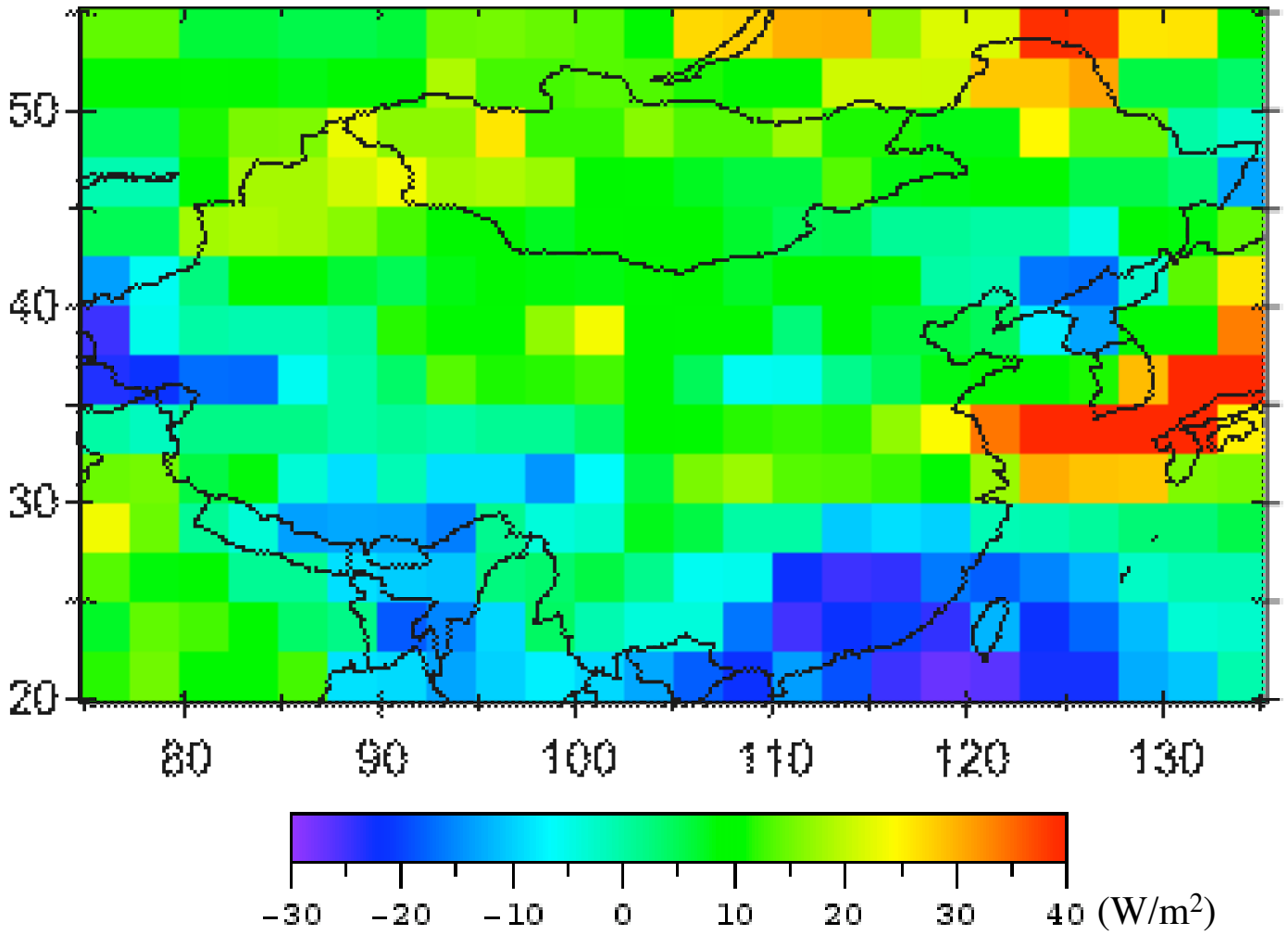

Figure 1c

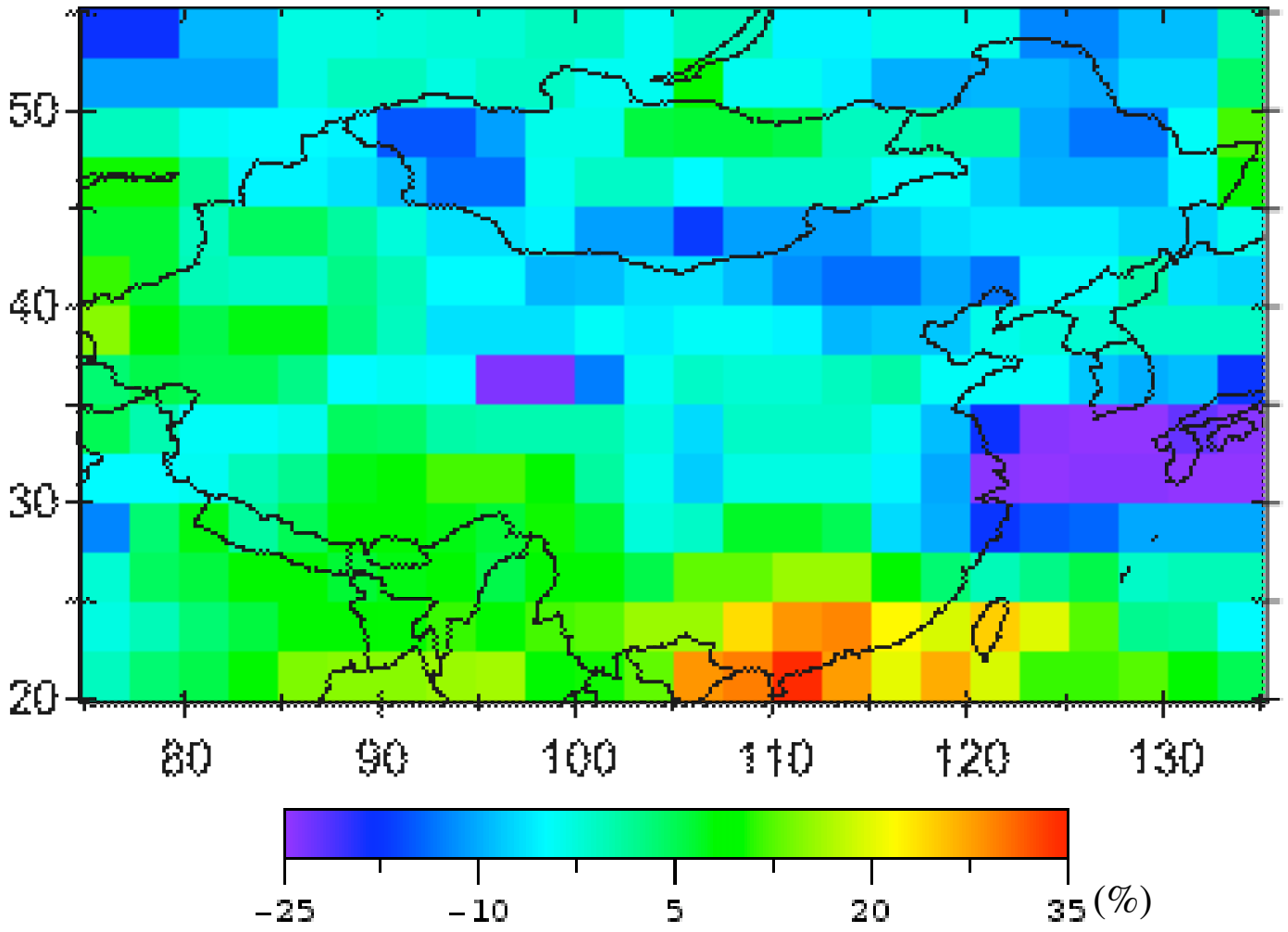

Figure 2a

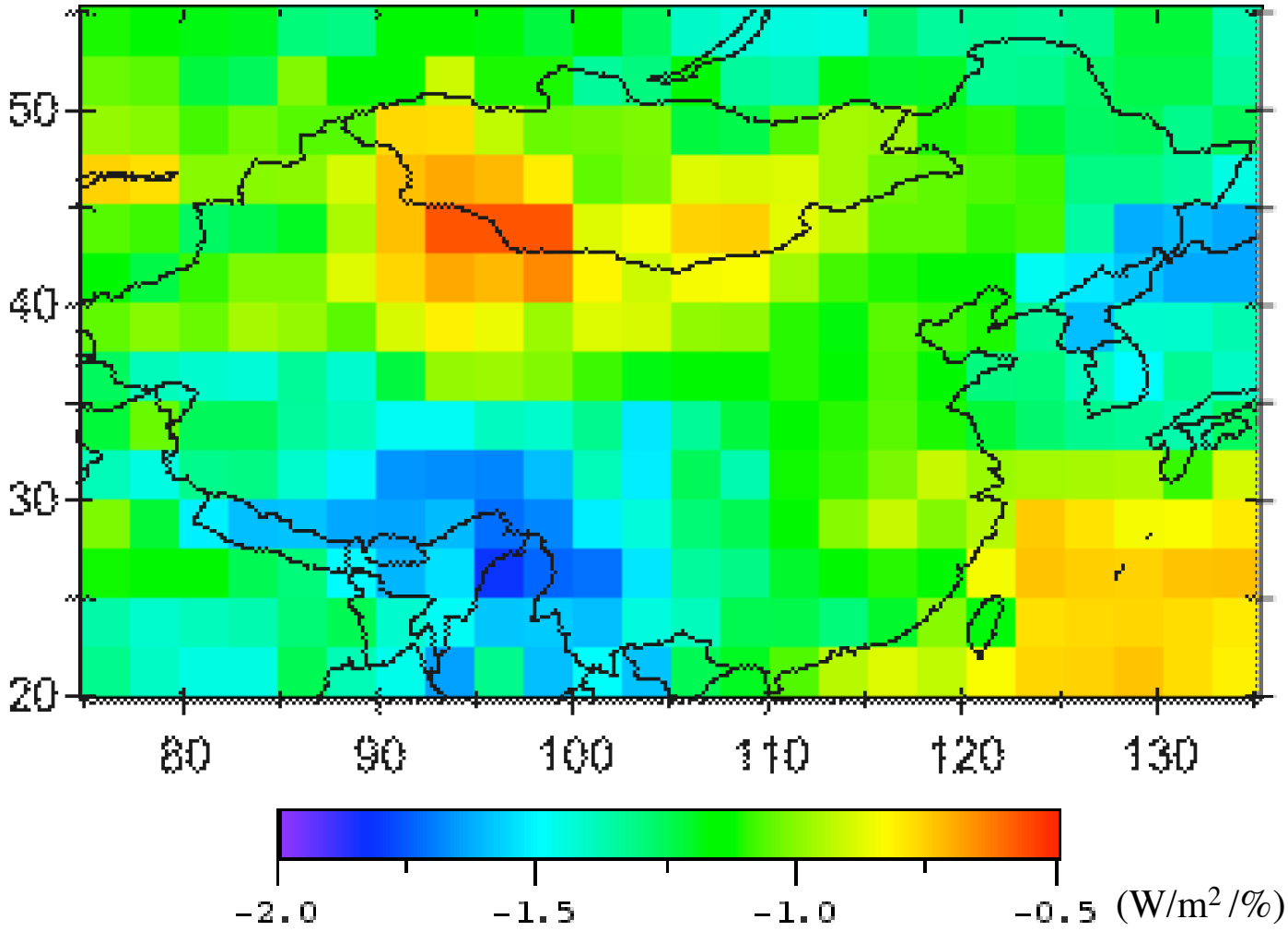

Figure 2b

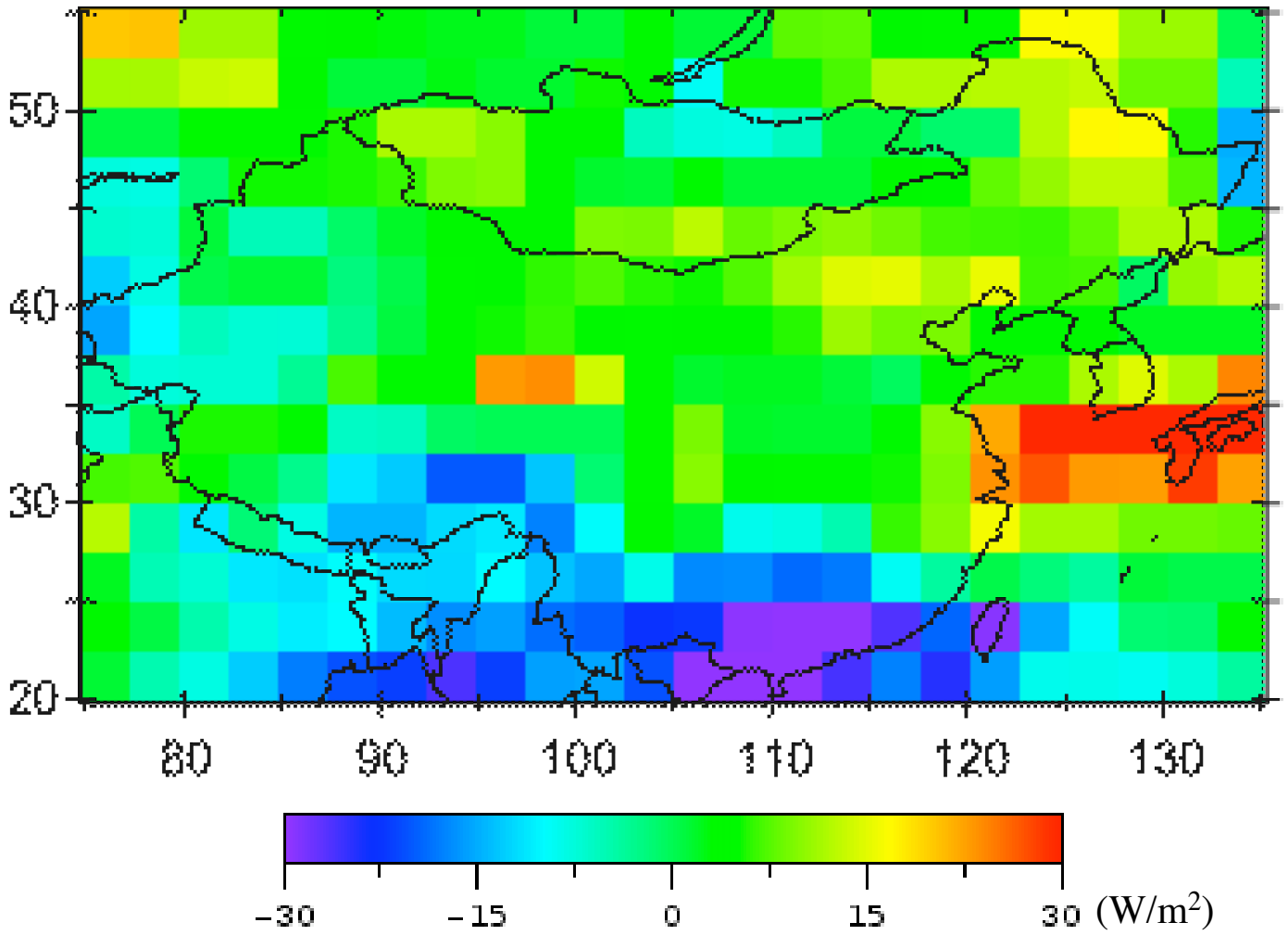

Figure 2c

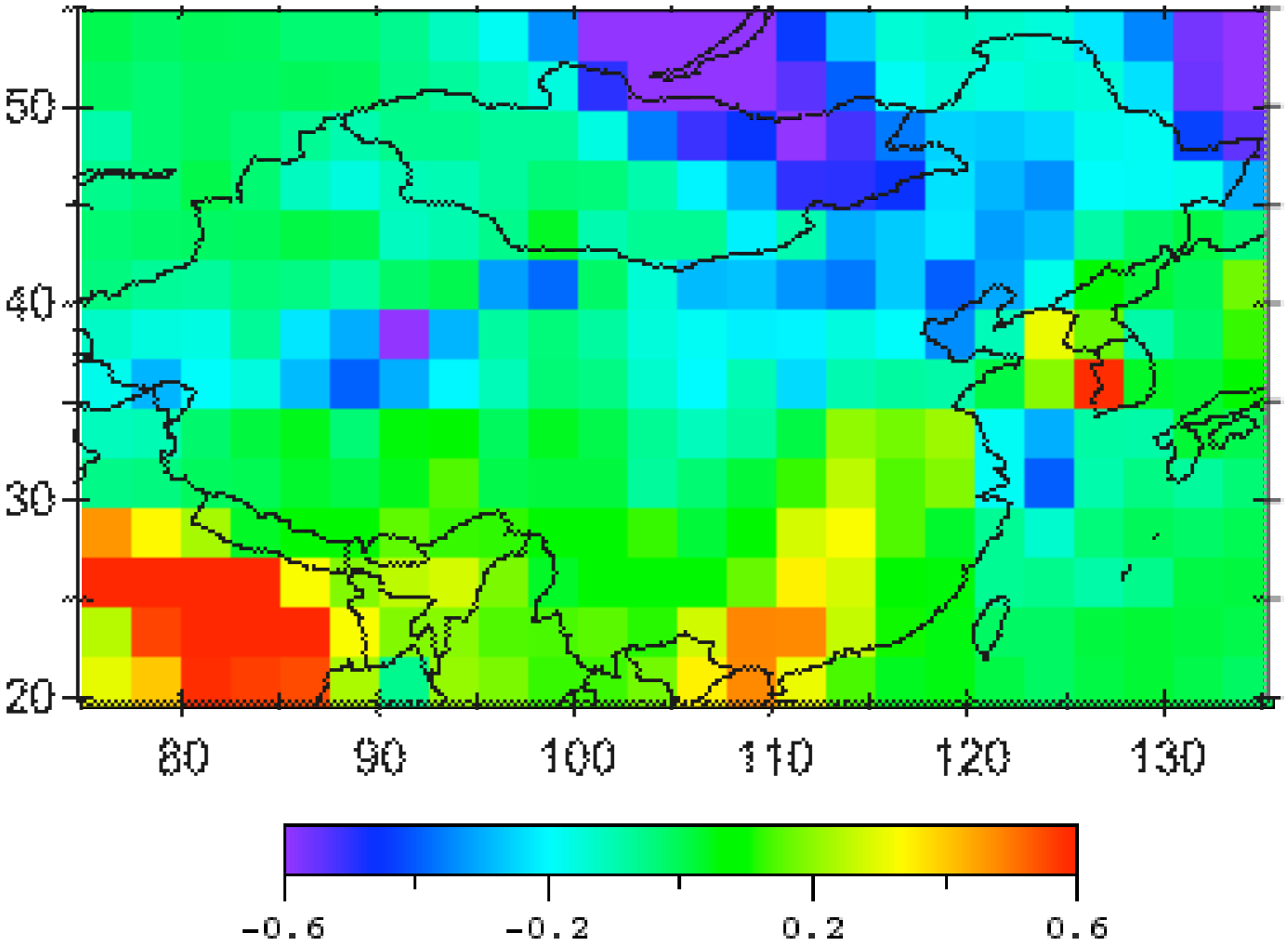

Figure 3a

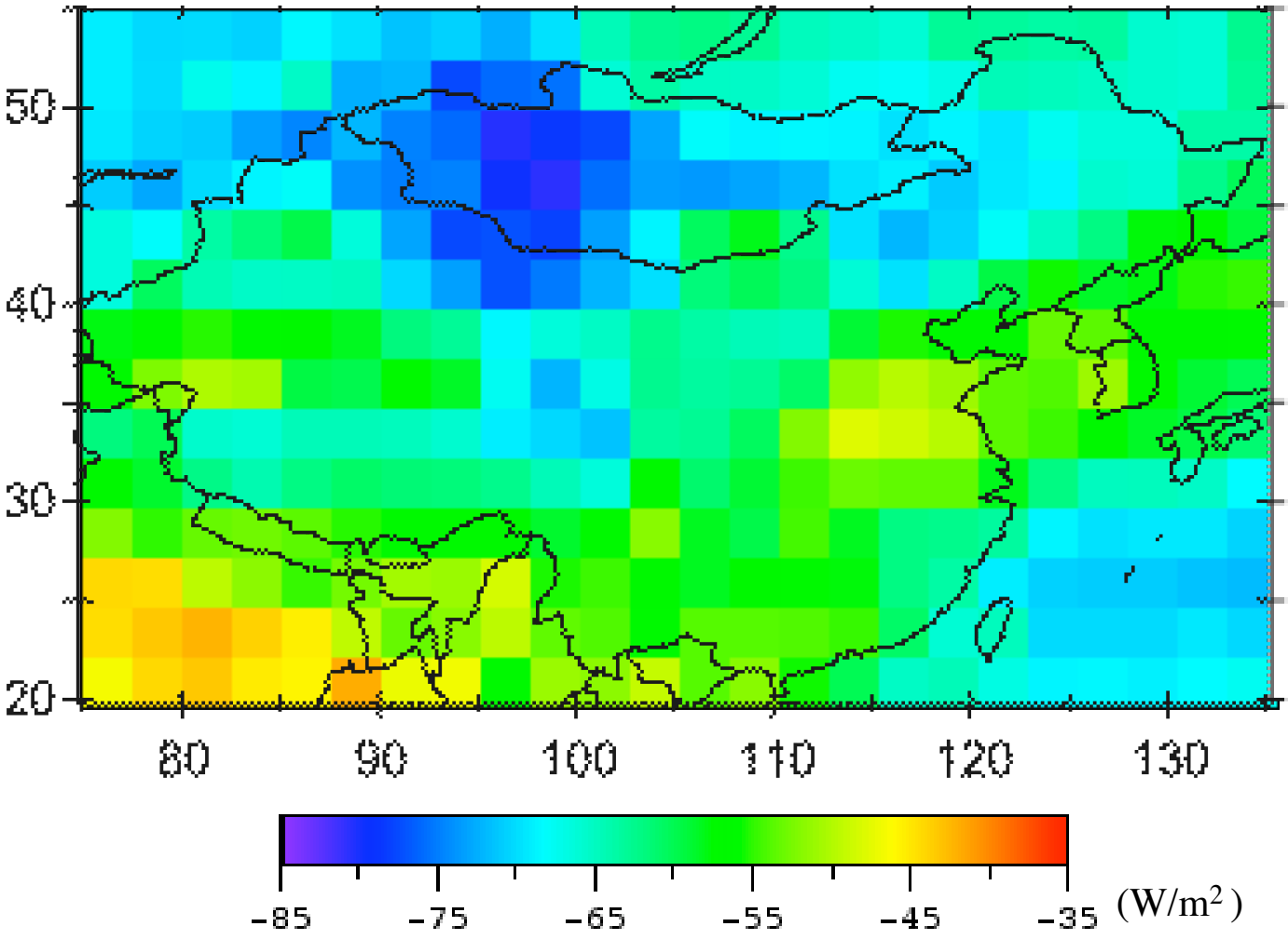

Figure 3b

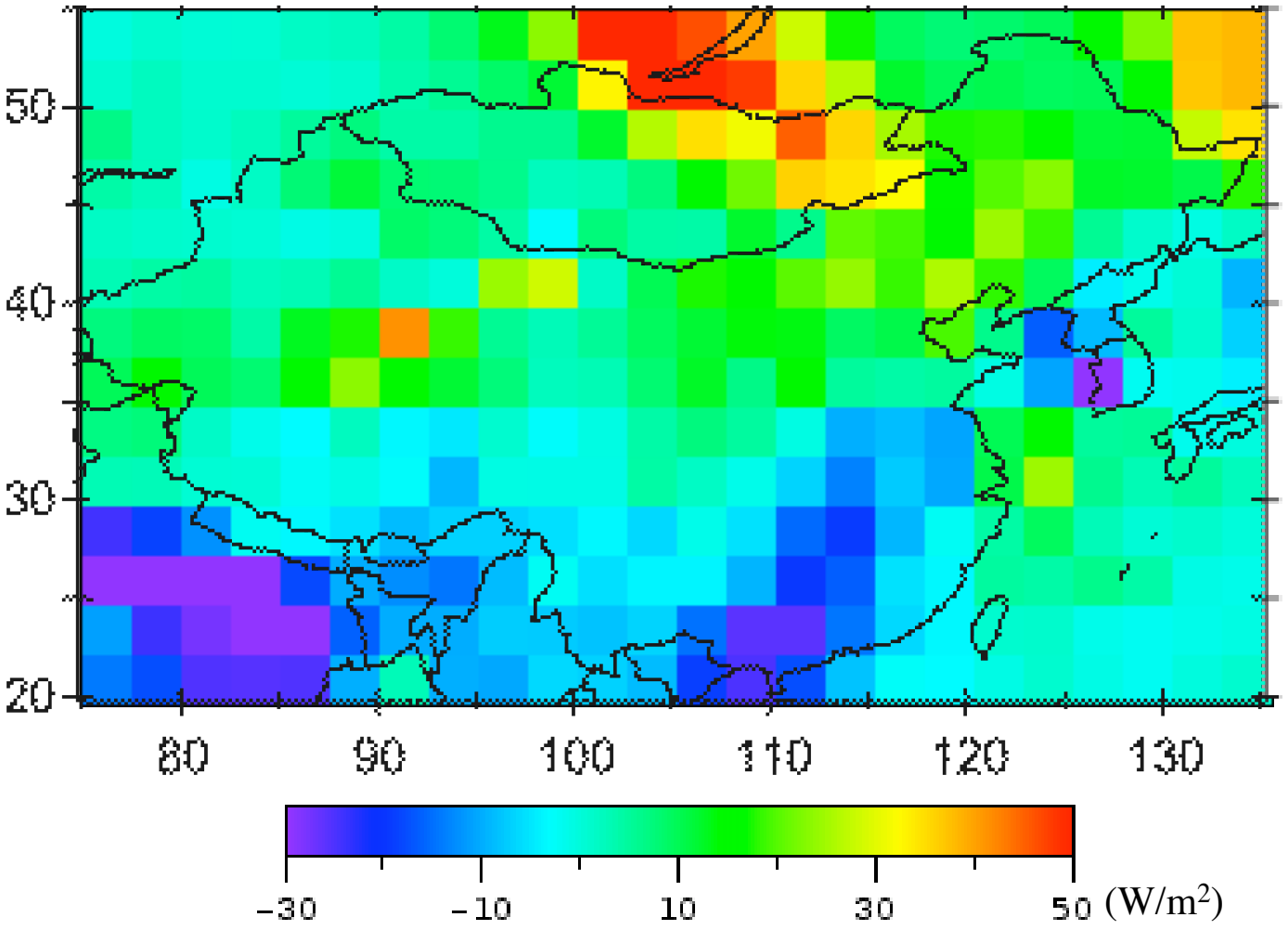

Figure 3c

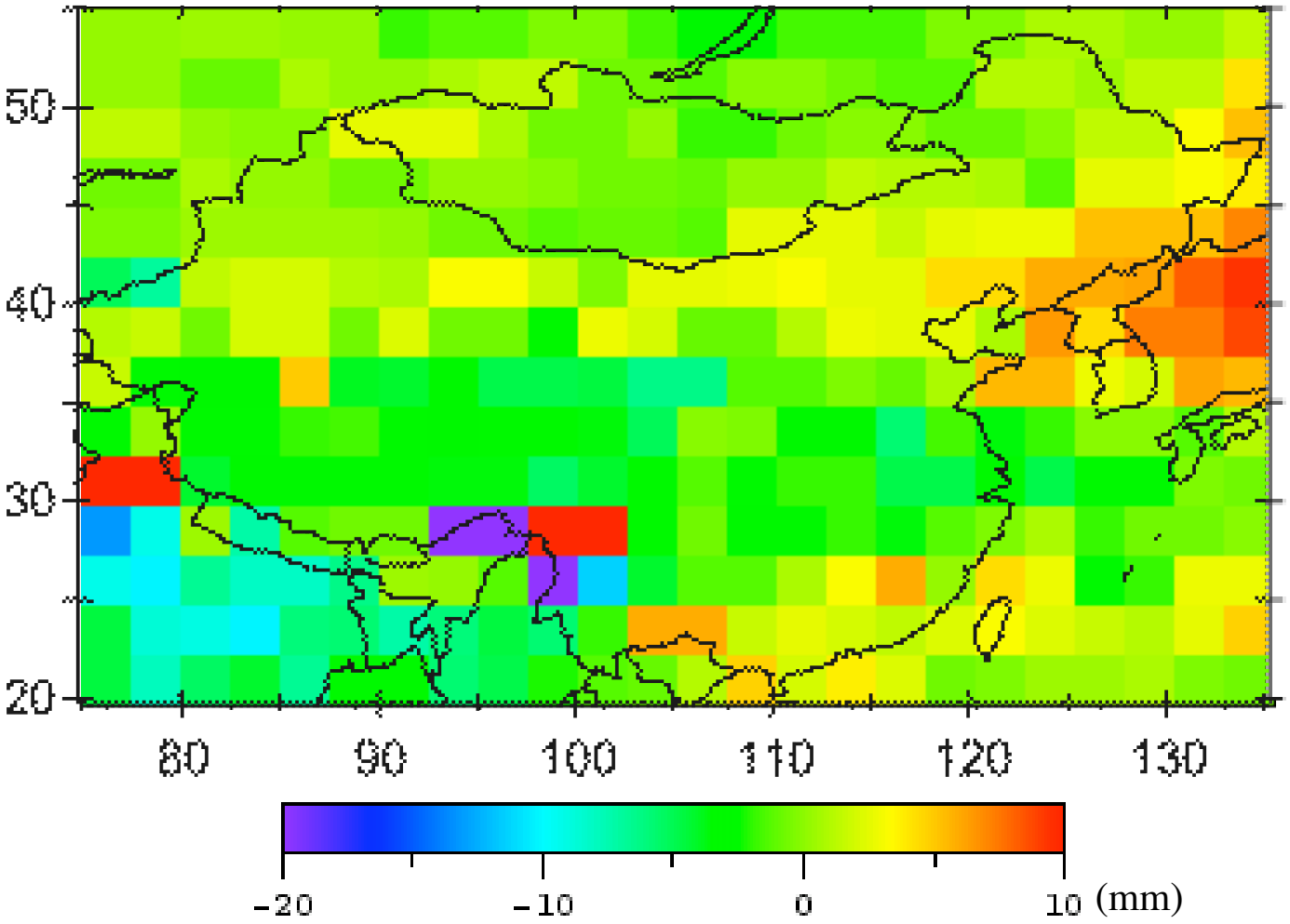

Figure 4a

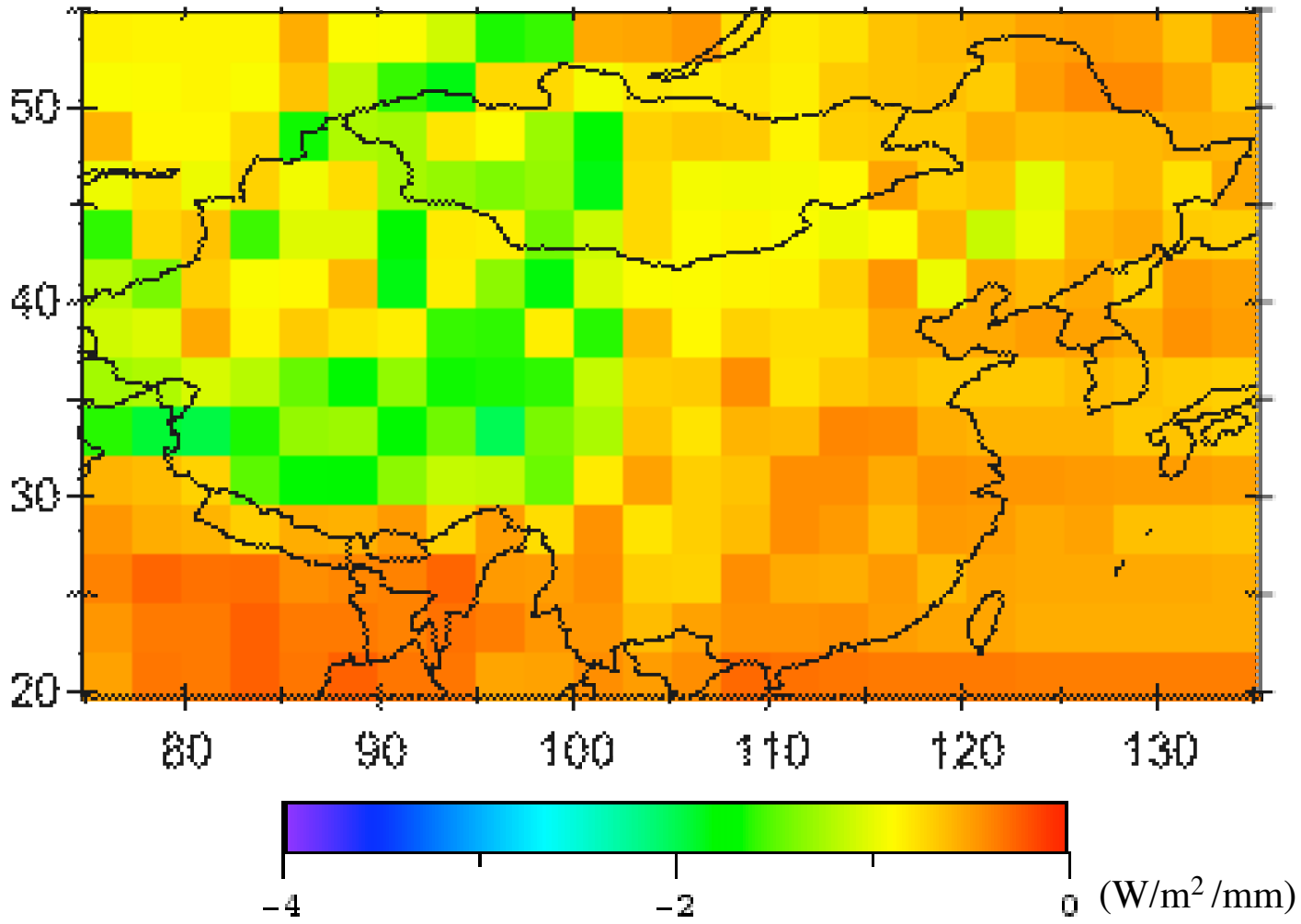

Figure 4b

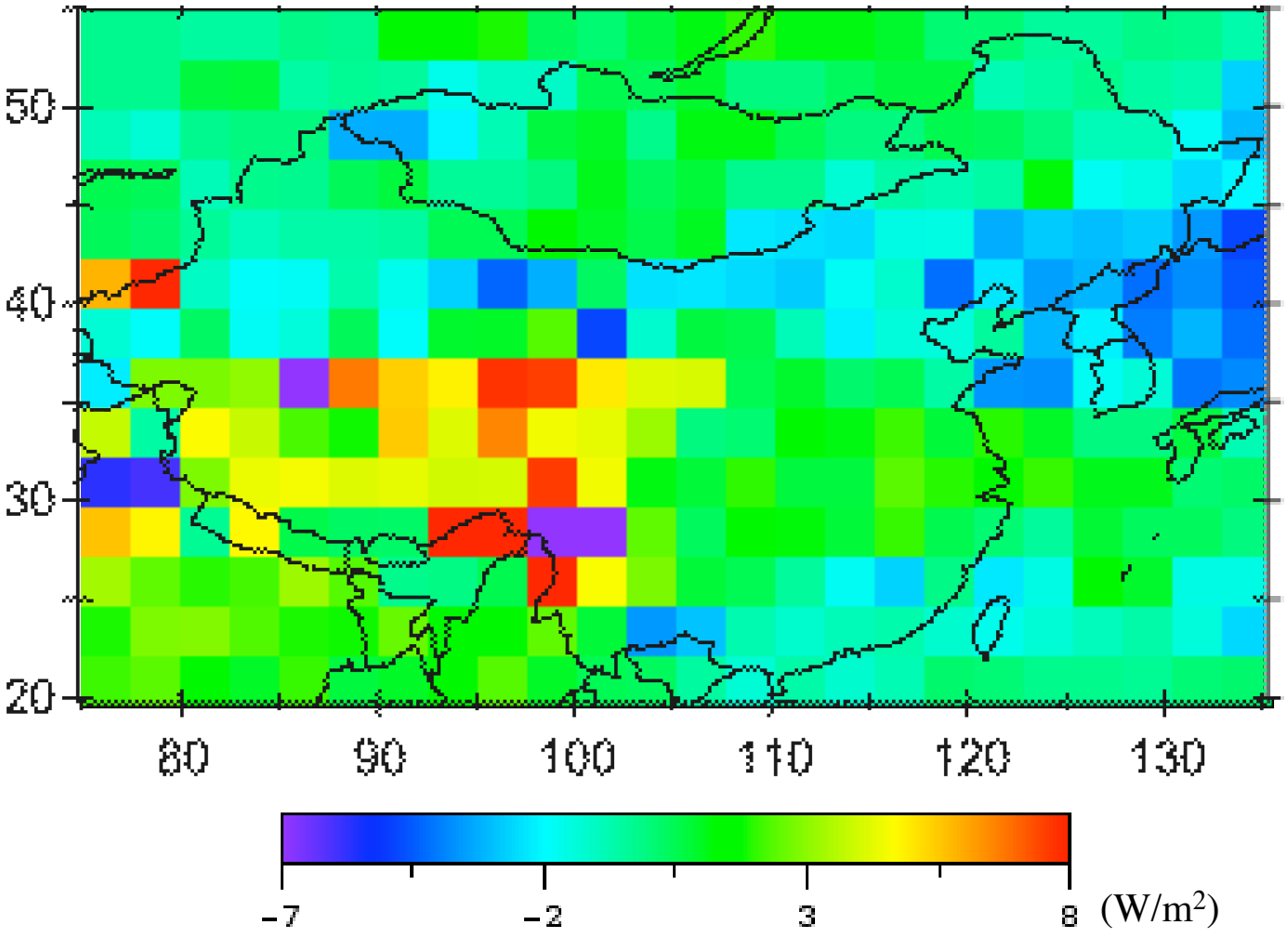

Figure 4c

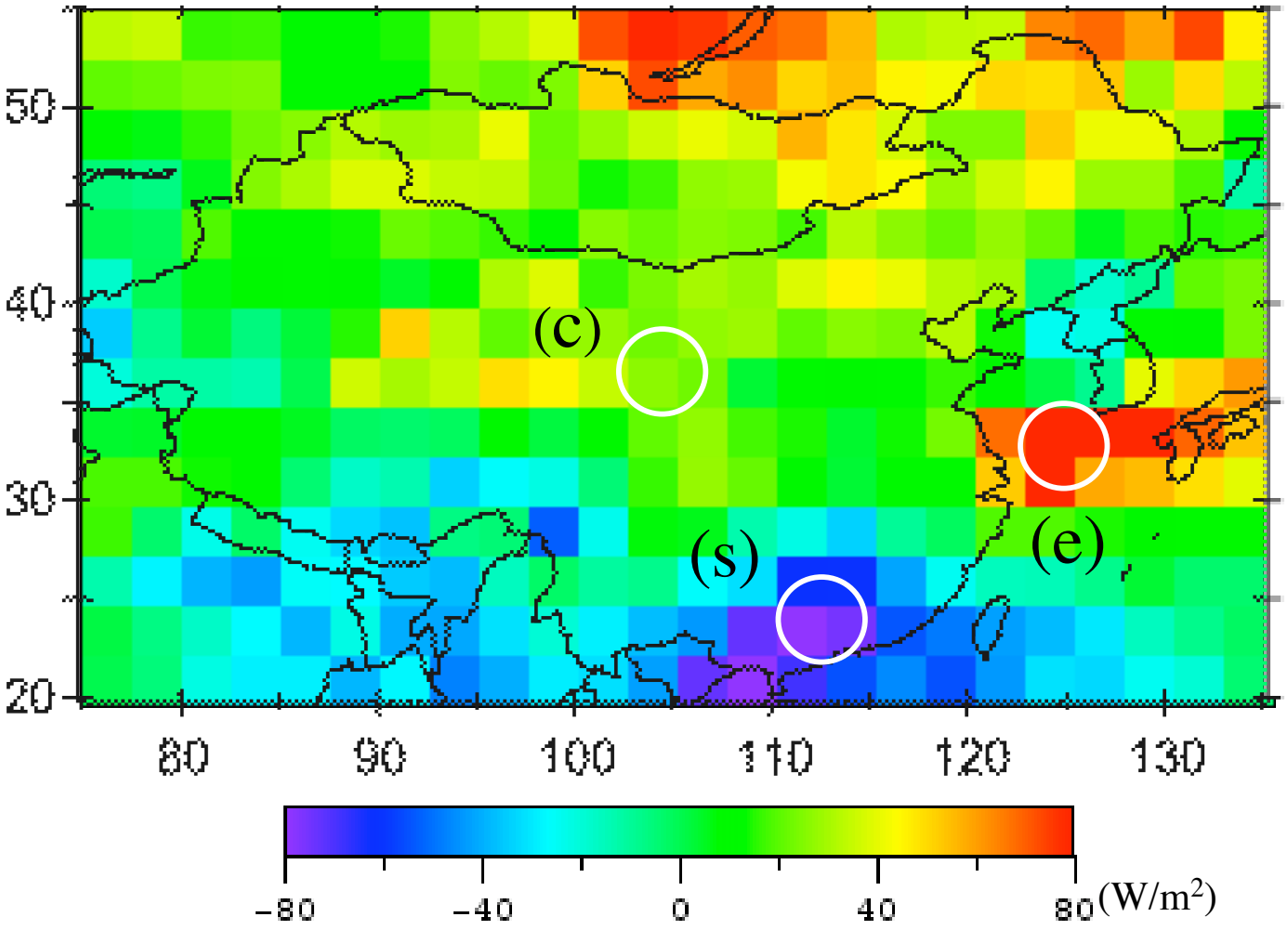

Figure 5

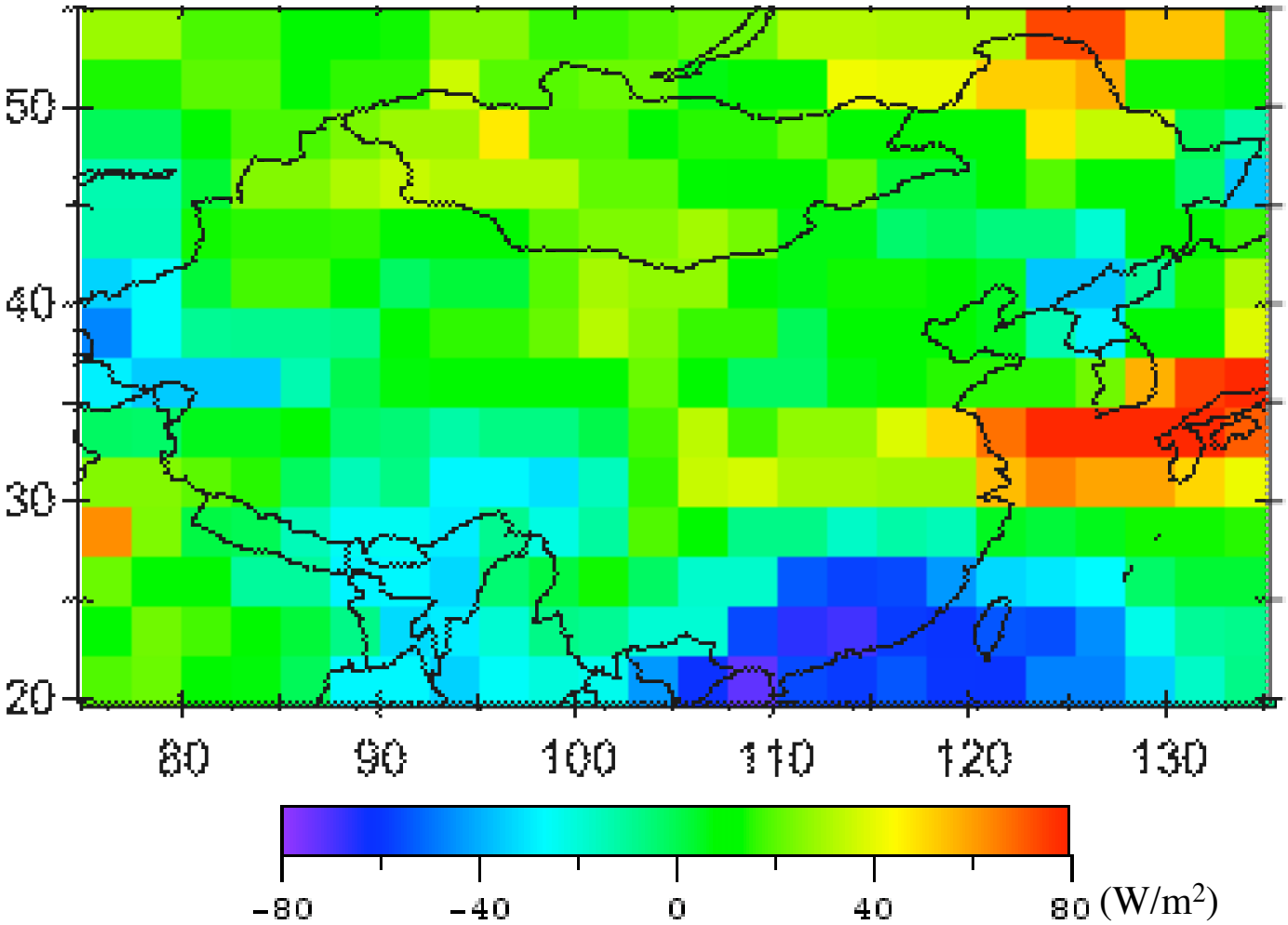

Figure 6

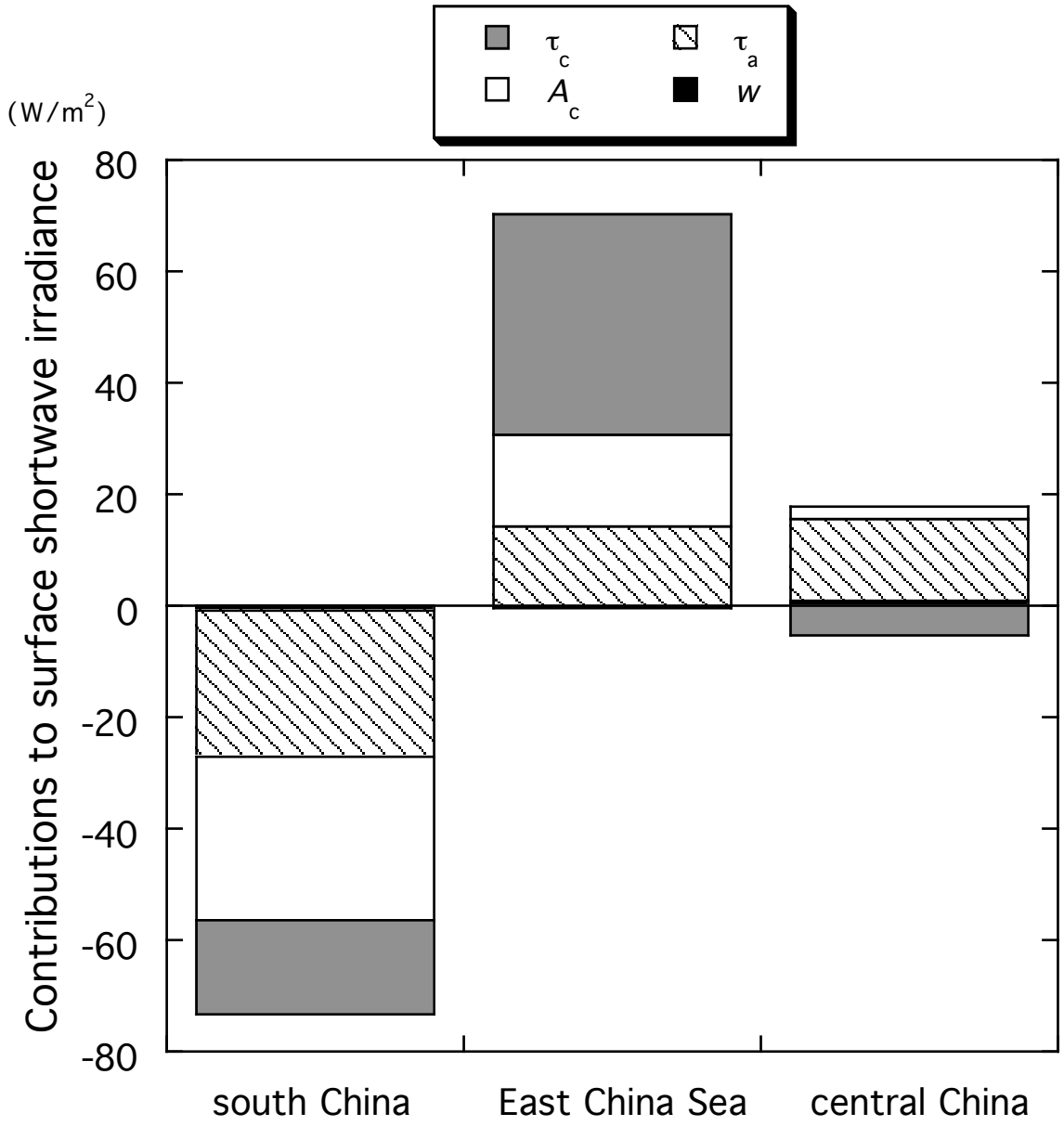
τc
τa
Ac
w
(W/m2)
Contributions to surface shortwave irradiance
80
60
40
20
0
-20
-40
-60
-80
south China
East China Sea
central China

Figure 7

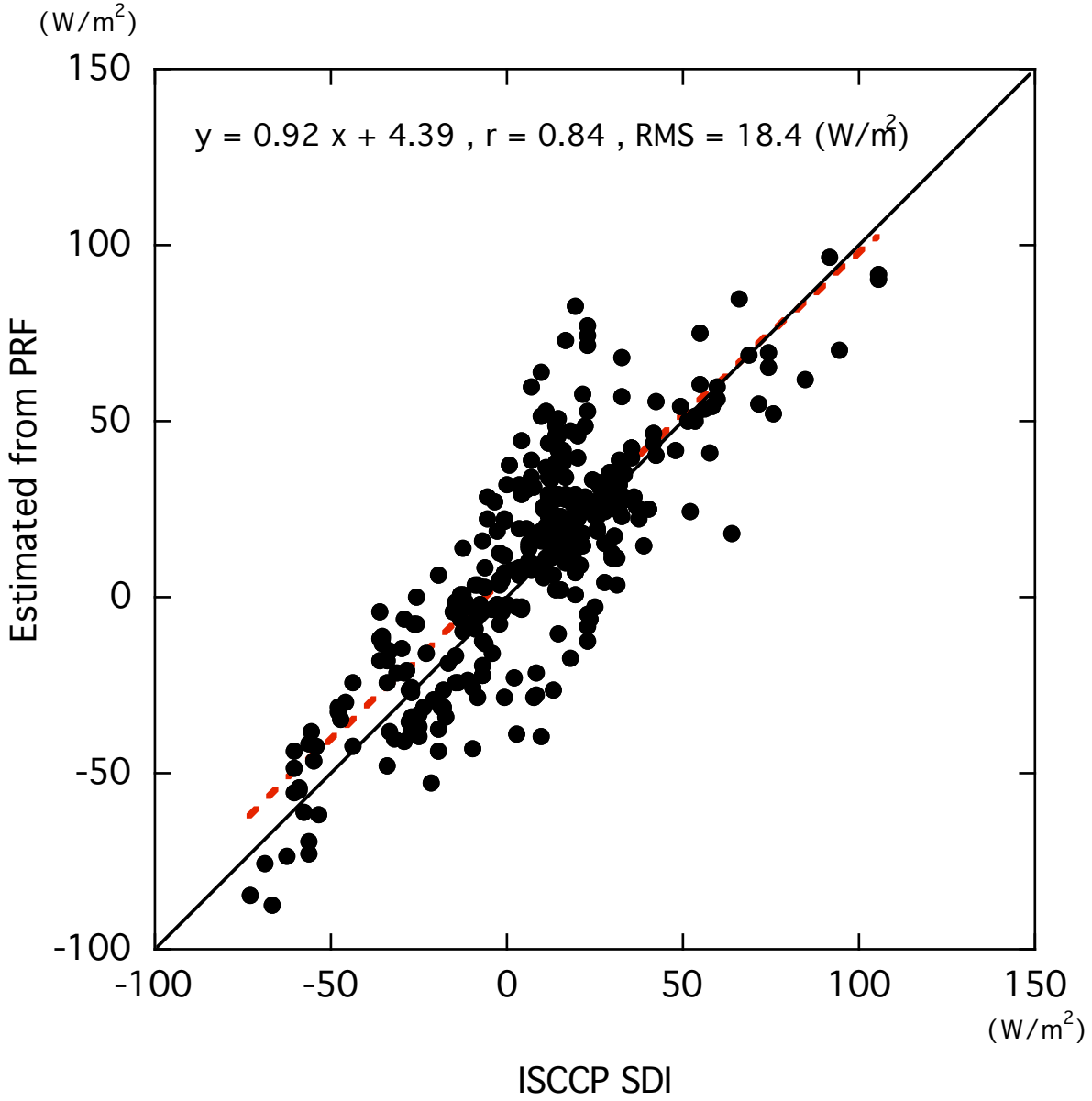
(W/m2)
150
100
50
0
-50
-100
y = 0.92 x + 4.39 , r = 0.84 , RMS = 18.4 (W/m2)
Estimated from PRF
-100
-50
0
50
100
150
(W/m2)
ISCCP SDI

Figure 8